SPIE Proceedings, Vol. 6368, in press (2006)

Near-field spectroscopic analysis of the mode structure in high-power diode lasers based on a double barrier separate confinement heterostructure

Anna Kozlowska*[a], Andrzej Maląg[b], Robert Pomraenke[c], Julien Renard[c], and Christoph Lienau[c,d]

[a]Institute of Electron Technology, 32/46 Al. Lotników St., 02-668 Warsaw, Poland;
[b]Institute of Electronic Materials Technology, 133Wolczyńska St., 01-919 Warsaw, Poland;
[c]Max-Born-Institut für Nichtlineare Optik und Kurzzeitspektroskopie, Max-Born-Str. 2A, 12489 Berlin, Germany;
[d]Carl von Ossietzky Universität Oldenburg, Institut für Physik, 26111 Oldenburg, Germany.

ABSTRACT

An analysis of the mode structure of high-power double-barrier separate confinement DB SCH diode lasers is presented. The devices are characterized by very low vertical beam divergence (13 – 22°, depending on the design version). Modelling of the fundamental mode distribution for three different design versions of DB SCH diode lasers is discussed and the results are compared to a macroscopic characterization of the devices (far-field directional characteristics and photocurrent spectra). Microscopic measurements of the near field distribution of these diode lasers with subwavelength spatial resolution are performed by employing a Near–field Photocurrent (NPC) technique. The mode structure of diode lasers is directly visualized giving indications about the interplay between the heterostructure design and the emission characteristics.

Keywords: High-power diode lasers, near-field photo current, NPC, double barrier separate confinement heterostructure.

1. INTRODUCTION

High-power diode lasers (DLs) are widely used as optical pump sources in solid state and fiber lasers. These applications require high-brightness, reliable sources with a good beam quality. Also, the requirements for the optical power delivered from a single device are constantly increasing. Such demands impose high energy densities at the diode laser facets, thereby increasing the risk of catastrophical optical damage (COD). This risk, however, can be diminished by an optimized heterostructure waveguide design [1,2].

The waveguide design influences both the optical field distribution at the facets, i.e., the near-field distribution and in the far-field. A 'tight' heterostructure waveguide design results in a near-field distribution in the form of a very narrow light emitting slot causing a high vertical beam divergence. The typical heterostructure design leading to such tight optical confinement is the single quantum well separate confinement heterostructure (SQW-SCH). Weakening of the confinement factor allows for spatially expanding the light spot at the facet, leading to a considerably enhanced level for COD. This can simply be achieved by enlarging the waveguide thickness. This solution is used in large-optical cavity (LOC) diode lasers [1,3]. A marked disadvantage of this approach, however, is the deterioration of the diode laser performance (e.g., a decrease of slope efficiency and T_0 value) when waveguides are designed excessively thick in order to reach very high power operation [1].

A solution which allows to simultaneously achieve both a high COD level and a low beam divergence with only moderate deterioration of DL performance is the double barrier separate confinement heterostructure (DB SCH) [2,4]. It

* kozlowsk@ite.waw.pl; phone 48 22 5487 931, fax 48 22 847 0631;
When this work was done the first author was with the Institute of Electronic Materials Technology.

contains thin, wide-gap barrier layers at the interfaces between waveguide and cladding layers that weaken the optical confinement, thereby increasing the radiation spot size at the laser facet and, concomitantly, decreasing the beam divergence. In the paper, three different design versions of DB SQW SCH structures are investigated. A theoretical and experimental analysis of mode structure in such laser structures is presented. Due to the small dimensions of the DL waveguide, an experimental determination of optical near-field distribution is practically impossible by the means of conventional microscopy. The diffraction limit of optical imaging can, however, be overcome by employing near-field optical spectroscopy (NSOM) [5,6]. The method allows for high-resolution characterization of optoelectronic devices. It was successfully used for analysis of spatial emission properties of diode lasers [7,8]. Direct imaging of optical mode profiles of diode lasers using near-field (NPC) photocurrent spectroscopy was demonstrated by Guenter *et al* [9]. In this paper, the NPC technique is used for experimental analysis of mode structure in DB SCH SQW diode laser structures. We demonstrate that the technique is capable of resolving even subtle changes in the optical mode profile and readily compared to quantitative theoretical modeling of optical mode profiles. This makes near-field photocurrent technique a viable, non-destructive method for characterizing and inspecting the waveguide design of high power diode lasers.

2. THEORETICAL

The double-barrier separate confinement heterostructure with a waveguide design enabling weaker optical confinement is schematically shown in Fig.1. Barrier layers 'inserted' at the interfaces between the waveguide cladding layers allow for separately controlling both carrier and optical confinement. According to the modeling, for suitable DBSCH design, a competition between guiding and antiguiding effects at the barrier interfaces leads to the antiguiding dominance compared to the primary waveguiding properties of a SCH SQW structure. This causes an expected weakening of the optical confinement, an enlargement of a light spot at the laser facet, and a vertical beam divergence ($\Theta_\perp$) reduction.

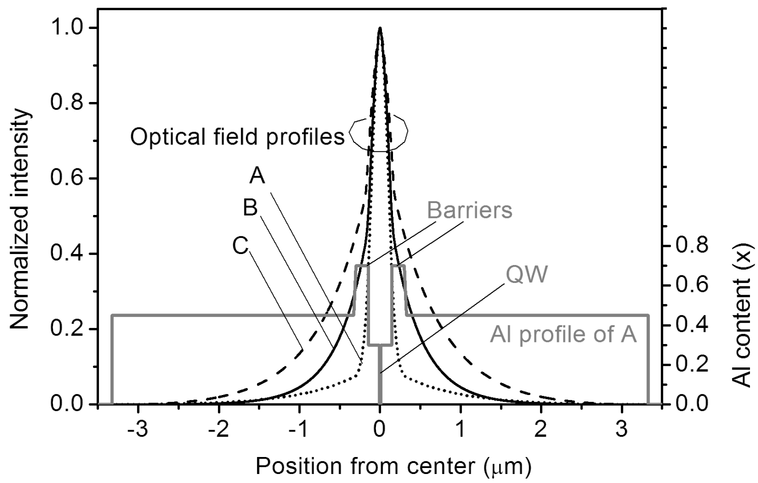

Fig. 1. Al-profile of the DB SCH diode (version A) and calculated optical mode profiles for three different variants of the heterostructure.

Three heterostructures, versions A, B, and C, have been designed. The layer sequence of an exemplary heterostructure (version A) is presented in Table 1. Versions B and C differ with respect to the waveguide and barrier thickness and composition. Modeling of the optical mode profiles for all three waveguides was performed using the commercial Photon Design software (Fig. 1). The optical mode profiles are non-Gaussian due to the formation of evanescent tails penetrating the claddings. These tails are relatively weak in amplitude for version A and much more pronounced for versions B and C. Calculated FWHM beam divergences are 15°, 13° and 12° for versions A, B and C, respectively.

	Layer	Composition x	Thickness	Dopant	Concentration [cm^{-3}]
13	GaAs - contact layer	0	0.3 µm	C	> 2E19
12	AlGaAs - p-cladding	0.45	2.4 µm	C	7E17
			~ 0.1 µm	C doping	gradient
11			0.5 µm	C	1E17
10	AlGaAs - gradient	0.7 → 0.45	30 nm	C	1E17
9	AlGaAs - barrier	0.7	150 nm	C	1E17
8	AlGaAs - waveguide	0.3	140 nm	u	-
7	GaAsP - QW	**for λ = 808 nm**	15 nm	u	-
6	AlGaAs - waveguide	0.3	140 nm	u	-
5	AlGaAs - barrier	0.7	150 nm	Si	~1E16
4	AlGaAs - gradient	0.45 → 0.7	30 nm	Si	1E17
3	AlGaAs - n-cladding	0.45	0.5 µm	Si	1E17
			~ 0.1 µm	Si doping	gradient
2			2.4 µm	Si	5E17
1	GaAs - buffer	0	~1 µm	Si	2E18

Tab. 1 Layer sequence of the double-barrier separate confinement heterostructure, version A.

3. EXPERIMENTAL

3.1 Diode laser structures

According to the scheme given in the previous section, three heterostructures (versions A, B and C) have been grown on a n-GaAs substrate by low pressure MOVPE. The tensile-strained 15 nm thick GaAsP quantum well was optimized for 808 nm emission [10]. The thickness, composition and strain of the heterostructure layers have been examined using SEM, PL, SIMS and XRD.

Wide-stripe gain guided laser structures were fabricated by He^+ implantation (E = 160 keV) [11]. The stripe width is 0.1 mm. TiPtAu and AuGeNi metallizations were applied as p- and n- contacts, respectively. Laser diode chips have been cleaved so that the cavity length L is 1 mm. The facets were HR/LR coated by sputtering with AlN-Si/AlN multilayers. The devices were mounted epi-side down on copper blocks. Three representative diode lasers, namely A, B, and C manufactured from the described earlier heterostructures, are investigated in this work.

3.2 Experimental setup

The experimental analysis of the mode structure in DBSQW diode lasers has been performed using an arrangement shown schematically in Fig. 2 [3,12]. A probe beam from a He-Ne or a tunable Ti-Sapphire laser emitting in the range between 780 and 820 nm is launched into a single mode fiber. The end of the fiber is tapered and metal coated so that a tip with an aperture of ~ 100 nm is formed. A chopper is used to modulate the probe beam with the frequency of 2.75 kHz. The tip is scanned at a constant distance (~ 10 nm) over the laser diode facet using a shear force feedback setup. The preamplifier photocurrent signal from the unbiased diode laser was detected by a lock-in amplifier.

Far-field directional characteristics have been recorded by a CCD camera corrected for the non-spherical detection surface [13]. Macroscopic photo-current spectra have been measured using a Fourier-transform spectrometer BRUKER IFS 66v. A more detailed description of this experimental arrangement can be found in Ref. 14.

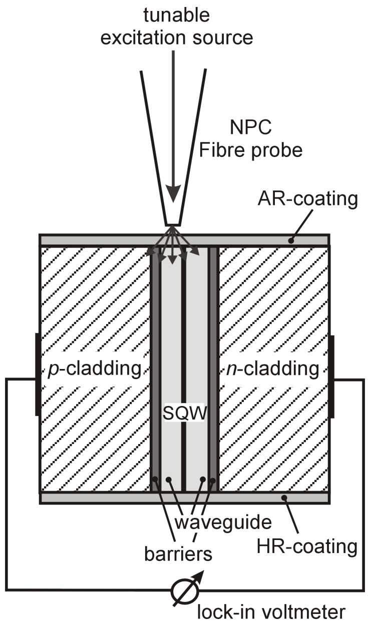

Fig. 2. A schematic of a Near-field Photo-current experimental setup [12].

4. RESULTS

4.1 Macroscopic characterization of diode lasers

The far-field directional characteristics in the plane perpendicular to the junction of the diode lasers A, B and C are shown in Fig. 3. The profiles are Gaussian-like and the vertical beam divergences (FWHM) are low for all devices under test (22°, 18° and 13° for the diode lasers A, B, and C respectively). They differ however slightly from theoretically predicted values, especially for structure A (calculated beam divergences are 15°, 13° and 12° for versions A, B and C, respectively).

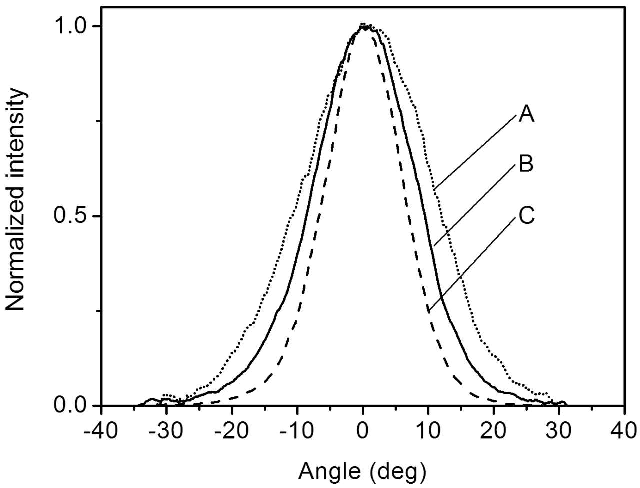

Fig. 3. Normalized vertical far-field profiles for diode lasers A, B and C.

Fig. 4 shows a macroscopic photocurrent spectrum of an exemplary diode laser (structure A). The signal increase at 1.53 eV results from interband absorption from the first hole level (light hole subband) to the first electron level in the QW. A local absorption edge at 1.85 eV, induced by absorption inside the laser waveguide, is also present. The small contribution from defect bands manifests itself in the weak shoulders at energies below 1.53 eV.

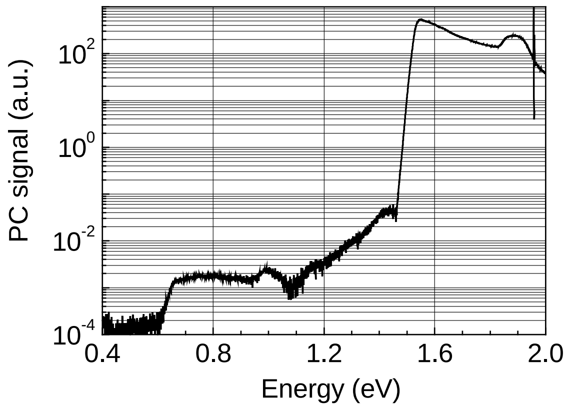

Fig. 4. Photocurrent spectrum in the below-band-edge region for a diode laser, version A.

The light-current characterization of the devices showed threshold current densities in the range of 250 – 280 Acm^{-2}, 270 – 300 Acm^{-2} and 300 – 350 Acm^{-2} and slope efficiencies of 0.75 W/A, 1.15 W/A and 0.95 W/A for A, B and C diode lasers, respectively. The slightly worse efficiencies of the A and C versions can be attributed to non-optimized doping during the MOVPE growth, while the 'intermediate' B-version proved to be the most insensitive to it. Series electrical resistances (measured at threshold current) were of the order of 0.15 Ω, and measured thermal resistances were in the range of 8 - 14 deg/W.

4.2 Microscopic (near-field) characterization of diode lasers

We first examine the dependence of NPC scans on the wavelength of the excitation beam. Here, a facet of the diode laser B was scanned in the direction perpendicular to the heterojunction with a probe beam that was tuned in wavelength between 633 and 820 nm. The resulting local photocurrent, plotted as a function of the local position (perpendicular to junction), is shown in Fig. 5. A maximum NPC signal can be observed in the area of DL active region (tip positions x = 0). The interface between heterostructure and substrate corresponds to the tip positions $x \cong 3$ μm.

It is evident that the main NPC signal comes from the photo-carriers generated by interband absorption inside the QW. For an excitation wavelength of λ = 633 nm - in addition to the QW absorption - also the $Al_{0.3}Ga_{0.7}As$ waveguide region contributes to the overall signal. This is consistent with the modeling results of the optical field distribution which indicate that for λ = 633 nm apart from a fundamental mode also higher order modes can be excited. For the wavelengths closer to DL emission (808 nm), the near field contains exclusively a fundamental mode as it can be observed in Figs. 5(b-d). Since the optically active QW layer with a thickness of 15 nm is much smaller than the dimension of the fundamental guided mode, the near-field photocurrent intensity essentially maps the coupling of the near-field radiation into the fundamental guided mode [9] and thus provides a direct measurement of the optical mode profile with subwavelength resolution.

FWHW of NPC line scans from Fig. 5(b-d) is plotted as a function of the excitation wavelength (Fig. 6). For longer wavelength, a slight broadening of the near-field profile can be observed. This broadening can be possibly attributed to the deeper penetration of the optical field into the laser structure [15].

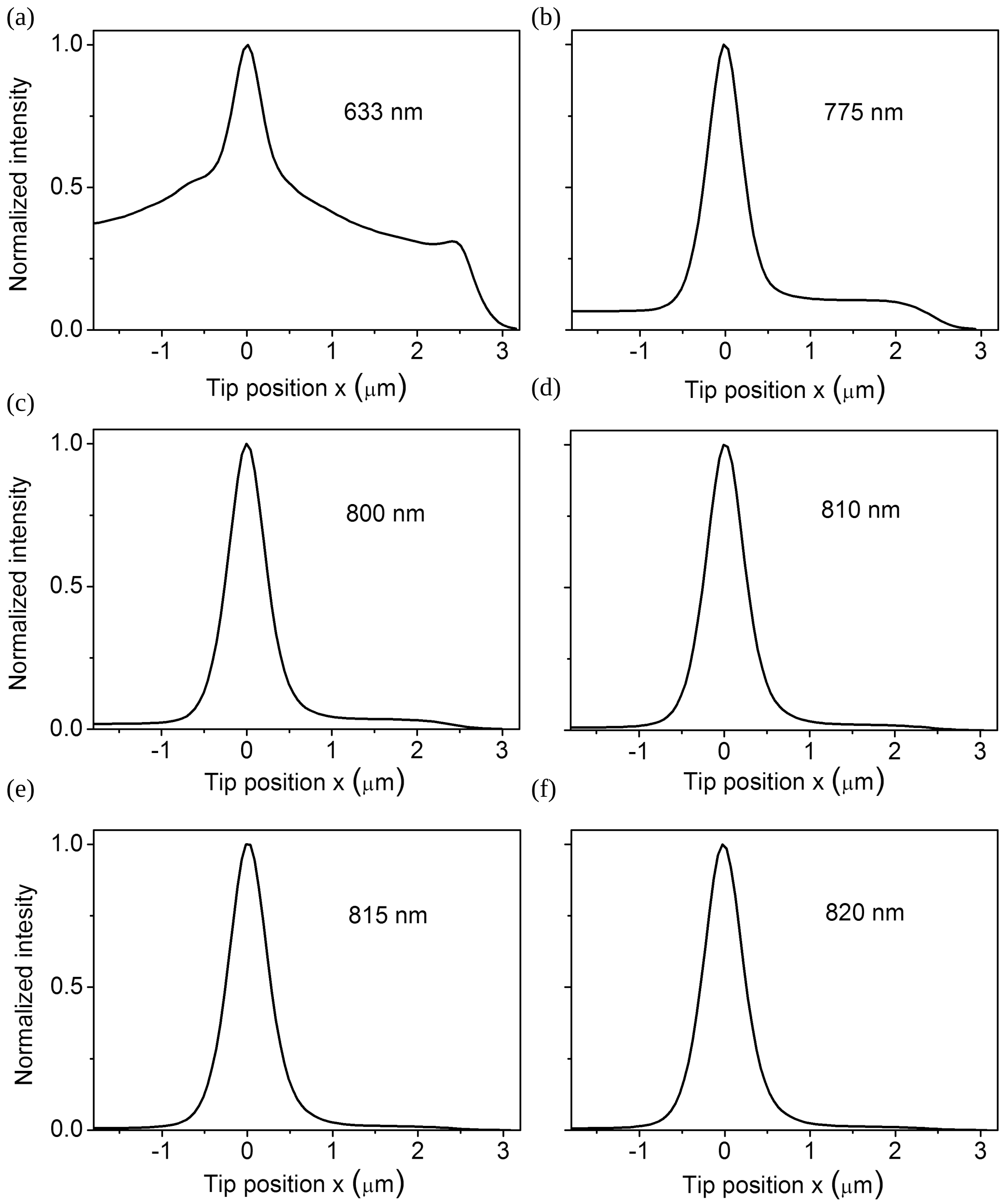

Fig. 5. NPC line scans in the direction perpendicular to junction for the diode laser B obtained with the different excitation wavelengths: 633 nm (a), 775 nm (b), 800 nm (c), 810 nm (d) 815 nm (e) and 820 nm (f).

The results of NPC characterization of the diode lasers A, B and C are shown in Fig. 7. The excitation wavelength (810 nm) was tuned close to the wavelength of DL emission. Thus, the mode profiles in DB SQW SCH diode lasers are directly imaged. The experimental results (open circles) are directly compared with the theoretical distributions of optical mode profiles (solid line, Fig. 7 d-f). There is nearly quantitative agreement between experiment and theory, especially when the FWHM of both traces is concerned. In particular, the near-field photocurrent data clearly reproduce the theoretically predicted width increase in the mode profile when going from structure A to C. This provides direct experimental evidence for the predicted tailoring of the optical mode profiles. A marked discrepancy between the experimental and theoretical results is the clear suppression of the evanescent tails in the experimental data. At present, we cannot definitely assign the physical origin for this effect. Most probably the real heterostructures differ slightly from the designed ones, as for layer thicknesses and compositions (Al-content). Also, the effect of the heterostructure doping on the optical mode profiles was not fully taken into account in the model calculations. The stronger waveguiding observed in the practically grown structures can be possibly be attributed to an Al-content in the barriers that is below the design value. We therefore anticipate that an optimization of this parameter should lead to an improved performance of DLs as far as the beam quality is concerned.

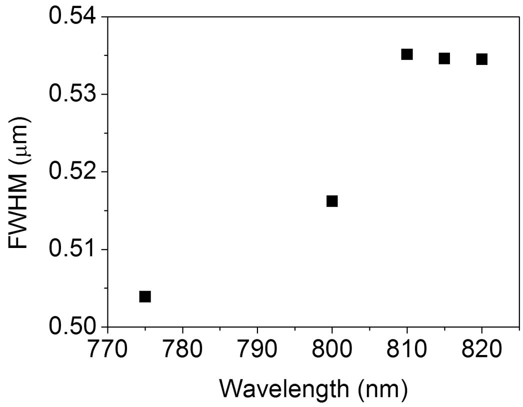

Fig. 6. FWHW of NPC line scans obtained with different excitation wavelengths for a diode laser B.

5. CONCLUSIONS

In summary, we have presented a mode profile analysis of high-power double-barrier separate confinement single quantum well DB SCH SQW diode lasers. Three different heterostructure versions have been analyzed both theoretically and experimentally. The results of a macroscopic characterization of the devices (far-field directional characteristics, photocurrent spectra) are given. Low vertical HWHM divergences (13 – 22^o, depending on the design version) have been achieved.

The Near-field Photocurrent technique was used to directly image optical mode profiles in DB SCH SQW laser structures. The experimental results have been compared with theoretical distributions of optical mode profiles and are essentially in quantitative agreement. In particular, the theoretically predicted variation in mode profile width is clearly resolved in the experiments. The desired tailoring of the optical model is thus clearly confirmed by the near-field photocurrent measurements, making this technique a powerful and non-destructive method for optical waveguide inspection in optoelectronic devices, specifically high power diode lasers. A remaining not yet fully understood discrepancy between the experimental and theoretical results, is the weak contribution from the evanescent tails of the mode profiles to the photocurrent signals. It can be possibly attributed to an Al-content in the barriers, which differs from the predicted value, as this is difficult to be characterized experimentally. An in-depth comparison between NPC experiment and theory will be reported elsewhere.

AKNOWLEDGEMNTS

The authors would like to thank Tran Quoc Tien for performing the macroscopic Fourier transform photocurrent measurement. This work was partly supported by the Polish Ministry of Science and Higher Education under the grant Nr. 4T11B00724 and by the Access to Research Infrastructures activity of the European Union, contract RII3-CT-2003-506350 EU.

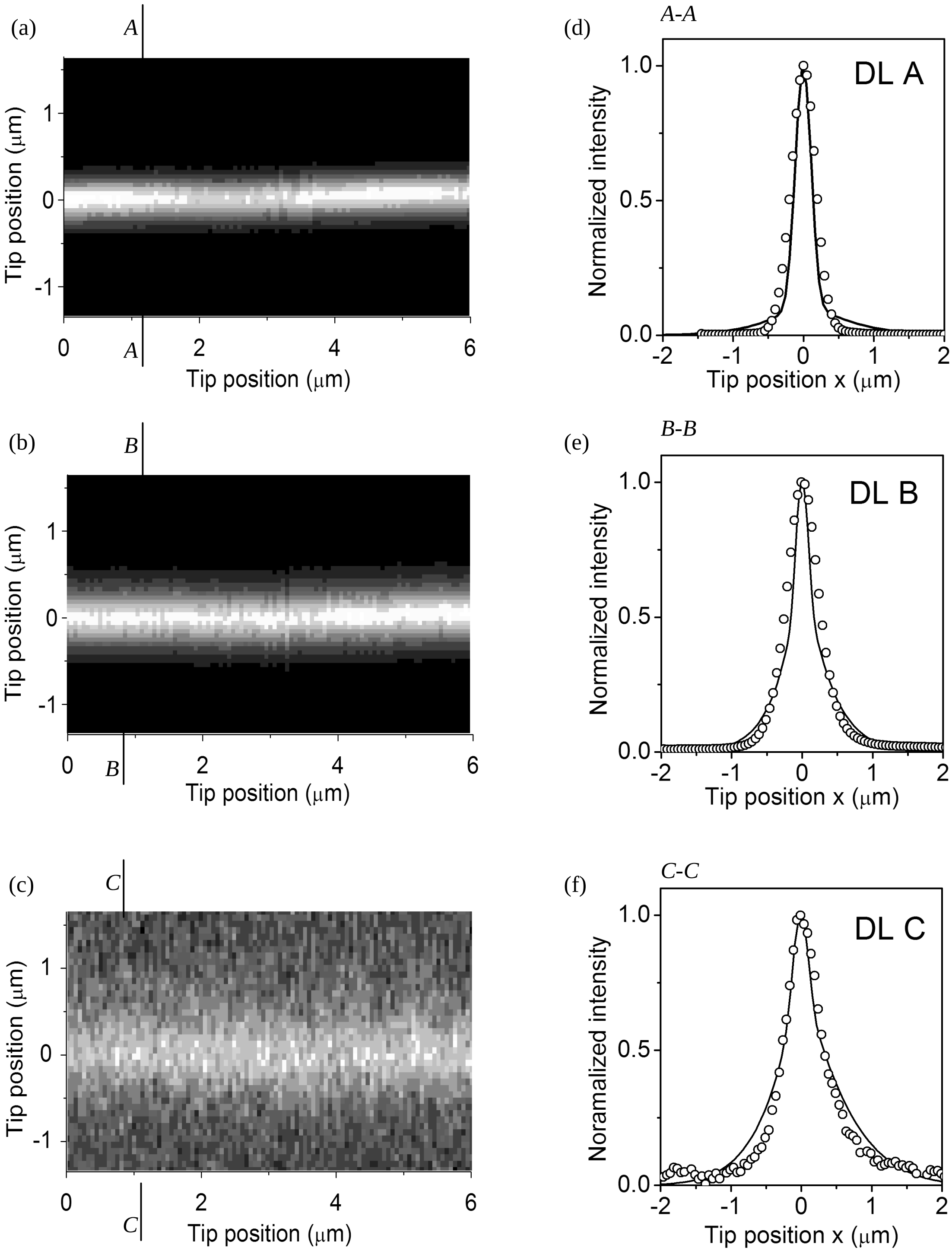

Fig. 7.(a-c) Two dimensional NPC image of a laser diodes A, B and C with DB SQW SCH heterostructure
(b-d) Cross sections of the NPC signal in the plane perpendicular to junction (open circles: experimental, solid line: simulation).

REFERENCES

1. A. Knauer, G. Erbert, R. Staske, B. Sumpf, H. Wenzel, M. Weyers, ”High power 808 nm lasers with a super-large optical cavity“, Semiconductor Sci. Technol., 20 (6), 621, 2005.
2. A. Maląg, A. Jasik, M. Teodorczyk, A. Jagoda, A. Kozlowska, ”High power low vertical beam divergence 800 nm-band double barrier-SCH GaAsP/(AlGa)As laser diodes, IEEE PTL, 18, 1582, 2006.
3. V. Malyarchuk, J.W. Tomm, T. Guenther, R. Müller, P. Kunkel, C. Lienau, J. Luft: „Large optical cavity waveguide for high-power diode laser applications“, Proc. SPIE, 4287, 11, 2001.
4. A. Maląg, B. Mroziewicz: „Vertical beam divergence of double barrier muliquantum well (DBMQW) (AlGA)As heterostructure lasers”, J. Lightwave Techn. Vol. 14, str. 514, 1996.
5. D.W. Pohl, W. Denk, M. Lanz: „Optical stethoscopy: image recording with resolution $\lambda/20$”, Appl. Phys. Lett., 44(7), 651-653, 1984.
6. E. Betzig, J.K. Trautman, T.D. Harris, J.S. Weiner, R.L. Kostelac: ”Breaking the diffraction barrier: optical microscopy on a nanometric scale”, Science, 251, 1468, 1991.
7. C. Lienau, A. Richter, A. Klehr, and T. Elsaesser, “Near-field scanning optical microscopy of polarization bistable laser diodes”, Appl. Phys. Lett. 69, 2471, 1996.
8. I. Hörsch, R. Kusche, O. Marti, B. Weigl, K.J. Ebeling: “Spectrally resolved near-field mode imaging of vertical cavity semiconductor lasers”, J. Appl. Phys., 79(8), 3831-3834, 1996.
9. T. Guenther, V. Malyarchuk, J.W. Tomm, R. Müller, C. Lienau: „Near-field photocurrent imaging of the optical mode profiles of semiconductor laser diodes“, Appl. Phys. Lett., 78 (11), 1463, 2001.
10. A. Knauer, F. Bugge, G. Erbert, H. Wenzel, K. Vogel, U. Zimmer, M. Weyers, “Optimization of GaAsP/AlGaAs-based QW laser structures for high power 800 nm operation”, J. Electron. Mat. **29**, 53, 2000.
11. A. Maląg: “Beam divergence and COD issues in double barrier separate confinement heterostructure laser diodes”, Bulletin of the Polish Academy of Sciences, 53 (2), 2005.
12. G. Behme, A. Richter, M. Süptitz, C. Lienau, “Vacuum near-field scanning optical microscope for variable cryogenic temperatures”, Rev. Sci. Instrum. 68, 3458, 1997 .
13. A. Kozlowska, M. Maląg, “Far-field emission characteristics of high-power laser diodes” Proc. SPIE, 5120, 178-183, 2003.
14. T. Q. Tien, J. W. Tomm, M. Oudart and J. Nagle, “Mechanical strain and defect distributions in GaAs-based diode lasers monitored during operation”, Appl. Phys. Lett. 86, 111908, 2005.
15. M.S. Ünlü, B.B. Goldberg, W.D. Herzog, D. Sun and E. Towe, “Near-field optical beam induced current measurements on heterostructures”, Appl. Phys. Lett. 67, 1862, 1995.